Results in Engineering 21 (2024) 101686

Contents lists available at ScienceDirect

Results in Engineering

journal homepage: www.sciencedirect.com/journal/results-in-engineering

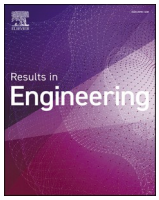

Estimating vehicle braking distance over wet and rutted pavement surface through back-propagation neural network

Jiaqi Jiang, Misagh Ketabdari *, Maurizio Crispino, Emanuele Toraldo

Department of Civil and Environmental Engineering, Politecnico di Milano, Piazza Leonardo da Vinci 32, 20133 Milan, Italy

ARTICLE INFO

Keywords:
Machine learning
Back-propagation neural network
Vehicle braking distance
Rutting
Dynamic skid resistance
Water film thickness

ABSTRACT

Due to repeated load cycles and climate impacts, road pavement deteriorates. One of the primary causes of pavement degradation is the formation of rutting under the wheel path on the road surface. Rutting's impact on vehicle performance, especially on rainy days (since the rain would fill the rutting depression), leads to longer braking distances compared to dry conditions. This study developed a MATLAB-based model for calculating vehicle braking distance on wet asphalt pavement affected by rutting, using dynamic skid resistances generated through Back-Propagation Neural Network (BPNN) analysis. This study addresses the worst-case scenario in which rutting is filled with water, then calculates the required vehicle braking distance under various Water Film Thickness (WFT) conditions. The developed model can perform these evaluations for different operational conditions across various input ranges, such as precipitation intensity, number of lanes, lane width, cross slope, average texture depth, rutting depths, and accumulated WFT. As an outcome, the vehicle braking distance can be estimated as a function of Rutting Depth (RD) within a known vehicle speed interval. After validating the proposed model against existing approaches from the literature, several sensitivity analyses are conducted to assess the impact of influencing parameters on the results. Moreover, the study examines the relationship between AASHTO braking distance requirements and the RD threshold levels adopted by several highway agencies. Furthermore, this model is also applicable to real-world case studies, enabling the calculation of vehicle braking distances with varying RDs in the presence of various WFTs on the pavement surface.

1. Introduction

Vehicle braking distance constitutes a significant portion of the total stopping distance, and its accurate determination is a fundamental necessity in the design of highways and urban roads. With today's improved understanding of the dynamic skid resistance mechanism, a more rational and mechanistic interpretation of vehicle braking distances can now be offered, connecting them with the tire-pavement skid characteristics (bituminous pavement texture). In essence, ensuring sufficient dynamic skid characteristics between the tire and the pavement is imperative for accurately calculating vehicle braking distances, thereby maintaining safe driving conditions across any road network.

Pavement rutting is a prevalent form of deterioration on road surfaces, resulting from repeated load cycles and environmental factors (high temperature). It is widely acknowledged by highway agencies and researchers that pavement rutting can diminish pavement surface performance, particularly in wet weather conditions, thereby posing safety risks such as hydroplaning and skidding. Consequently, there is a pressing need to establish an analytical model for estimating vehicle braking distances on wet and rutted pavements, to comply with road safety standards.

The current challenge in assessing the impact of Rutting Depth (RD) on vehicle braking distance on wet asphalt pavement lies in determining effective skid performance between the tire and pavement. This is particularly complicated by variations in water accumulation under different RD severity conditions. Existing literature highlights a scarcity of data on the dynamic skid performance within significant intervals of Water Film Thicknesses (WFTs), such as those ranging from 10 to 35 mm. Additionally, there is a lack of clarity on how to measure the influence of RD on vehicle braking distance in wet pavement conditions. This information is crucial for establishing the threshold RD level necessary to comply with road safety standards in pavement maintenance and rehabilitation.

To tackle these challenges, this study develops an analytical model designed to simulate tire-fluid-pavement interactions. Its primary objective is to assess vehicle braking distance on wet pavement under

* Corresponding author.
E-mail address: misagh.ketabdari@polimi.it (M. Ketabdari).

https://doi.org/10.1016/j.rineng.2023.101686
Received 28 November 2023; Received in revised form 6 December 2023; Accepted 13 December 2023
Available online 17 December 2023

the influence of rutting. The study considers various boundary conditions, including intense precipitation, the number of road lanes, lane width, road cross slope, pavement average texture depth, RD, and accumulated WFT (ranging from 0 to 35 mm). Moreover, vehicle speed, ranging from 0 to 100 km/h, is considered in the analysis.

2. Literature review

Stopping distance represents a crucial road safety requirement, as it signifies the minimum distance required for a vehicle to come to a complete stop. However, measuring stopping distance in the field can be both energy and time-consuming, mainly due to the presence of various environmental uncertainties. According to American Association of State Highway and Transportation Officials (AASHTO) recommendations [1], mechanical principles are employed to calculate stopping distance, making the tire-pavement friction coefficient a pivotal factor in determining braking accuracy.

In the latter half of the 20th century, the knowledge of tire-pavement skid resistance primarily relied on experimental data and observations in the absence of a comprehensive understanding of complex tire-fluid-pavement interactions. In early 1960s, the British pendulum tester was first popularized in the UK for low-speed skid resistance measurements of in-service pavements [2]. Then a significant breakthrough in skid resistance development occurred with the conduct of full-scale experimental tests by the National Aeronautics and Space Administration (NASA) and the Federal Aviation Administration (FAA) [3]. Vehicle skidding and hydroplaning were first assessed encompassing the influence of tire properties, WFT, and pavement conditions. Subsequently, extensive research and studies have been undertaken, mainly through field and laboratory experiments [4–6]. These experiments have resulted in the derivation of numerous empirical relationships to express pavement skid resistance. Regrettably, these empirical relationships have proven inadequacy for predicting pavement skid resistance in pavement engineering due to their limited vehicle operation conditions.

The early 2000s witnessed a significant advancement with the advent of high-speed computers and available numerical software. This progress enabled the prediction of skid resistance under diverse vehicular operating conditions, WFT variations, and pavement characteristics. Researchers started employing computer simulation models to address the tire-pavement skid resistance issue, particularly concerning vehicle speed and WFT, while also factoring in measured values [7–9] and the matter of hydroplaning speed on wet pavements garnered attention [10–12], the results are validated with the previous experiments and field measurements.

A noteworthy development came from the National University of Singapore (NUS) research group, which pioneered efforts to tackle wet-weather pavement skid resistance and hydroplaning issues using finite element computer software ADINA in 2005 [13]. They deviated from traditional approaches, which relied on statistical predictive equations or estimated ground friction values. Instead, they proposed an analytical simulation model grounded in engineering mechanics and fluid dynamics theory to calculate wet-pavement aircraft braking distance.

Furthermore, stopping distance has been incorporated into pavement management systems to improve road safety and operational efficiency, in accordance with mechanistic principles [14]. The tire-pavement friction coefficient plays a crucial role in the calculation of stopping distance. The model developed by Chu and Fwa monitors the available skid resistance across a range of WFT (i.e., 0–10 mm) and vehicle speeds (20–100 km/h). It's worth noting that each skid simulation analysis generated by their model is quite time-consuming.

In 2011, Pasindu et al. [15] enhanced the procedure for calculating wet-pavement braking distance based on the 3D tire-fluid-pavement model developed by Fwa and Ong [7,8]. They considered the intricate relationship between wet-pavement skid resistance and various aircraft operating conditions, which encompass aircraft tire type, landing speed (i.e., 20, 30, 40, 45 m/s), wheel load (i.e., 10, 25, 50 KN), tire inflation pressure, and WFT (i.e., 1, 2, 5, 10 mm). This model underwent validation using measured data by Horne et al. [16].

In 2019, the group of researchers involved in this study (Ketabdari et al. [17]) introduced a comprehensive aircraft risk model based on the probability of excursion accidents and an aircraft braking distance model proposed by Pasindu et al. [15]. Within this model, they developed five distinct MATLAB codes for simulating runway braking distance under varying conditions, encompassing different weather conditions, WFT, aircraft weight, and touchdown speed probability distributions.

During years 2020 and 2021, Ketabdari et al. [18,19] further improved the previous aircraft braking distance model, factoring in the impact of longitudinal and transverse slopes on aircraft braking distance under wet pavement conditions, as well as their influence on the probability of landing overrun accidents.

On the other hand, pavement rutting is a common pavement distress, often occurring in both bituminous bonded layers and underlying unbound layers [20]. In 2012, Fwa et al. classified rutting severity (i.e., 5, 10, 15, 20, and 25 mm) based on threshold values, hydroplaning risk, and the required braking distance at specific speeds (i.e., 50–100 km/h) [21]. In 2016, Pasindu et al. conducted an analysis of the effect of rutting depths (i.e., 5, 10, 15, and 25 mm) on aircraft hydroplaning risk in flooded pavement conditions [22], utilizing the well-established 3D tire-fluid-pavement model developed by Fwa and Ong [7–9].

In 2023, the authors of this paper (Toraldo et al.) investigated the impact of airport runway RDs, ranging from 1 to 26 mm, on aircraft landing braking distance [23]. This analysis considered dynamic skid resistance under heavy precipitation. The model used in this research was validated using examples developed by Pasindu et al. [15].

Machine learning is rising as a new technology of artificial intelligence and has been used in civil engineering in recent years. In 2022, Nyirandayisabye et al. [24] detected pavement distresses, specifically emphasis on rutting, cracks and roughness level by comparing the various regression machine learning algorithms. In 2023, Pan et al. [25] proposed a generative adversarial network to segment pavement cracks automatically, which diminished the effect of noise and segments cracks with more details. However, data scarcity is the main issue in civil engineering field due to experiments and data collection process are quite time-consuming and difficult. In 2023, Chen et al. [26] proposed to expand the liquefaction data set using wasserstein generative adversarial networks, after enhancing the training dataset, support vector regression, random forest, naive byes, and K-nearest neighbor were used to validate the improved accuracy of proposed model.

As concluded from the existing literature in the field, there have been no studies addressing the influence of RD on vehicle braking distance under intense precipitation on road pavement. This study aims to fill this knowledge gap.

3. Methodology

The model proposed in this study comprises four sub-models designed to assess the impact of RD on vehicle braking distance under intense precipitation, representing the worst-case scenario where the ruts are filled with water. These integrated sub-models collectively yield the final results for vehicle braking distance on wet and rutted pavements.

The first sub-model employs the WFT empirical formula developed by Gallway et al. [27] to determine the thickness of existing water film over the wet, but undeteriorated pavement surface during precipitation. For this matter, input parameters include average texture depth, drainage-path length, rainfall intensity, and cross slope.

On the other hand, rutting is a significant pavement surface distress that can alter drainage pathways and create water pooling areas. In this regard, the second sub-model assumes a transversal rectangular rut shape, where the RD remains constant within each rut, and the WFT at the rut position is the sum of RD and WFT over the undeteriorated

pavement surface.

The third sub-model introduces an innovative approach by employing Back-Propagation Neural Network (BPNN) algorithms to simulate dynamic skid resistance based on existing data according to the literature, offering a novel contribution to this study. In fact, BPNN is chosen after comparative investigation with Random Forest (RF) algorithm.

In the final step, the output from the first three sub-models serves as input for calculating vehicle braking distance on a wet and rutted pavement surface, as executed in the fourth sub-model.

3.1. WFT calculation model on undeteriorated pavement surface

Over the past years, several empirical and analytical formulas have been developed to calculate the WFT on the pavement surface under specific rainfall intensities. In sub-model 1, the formula developed from experimental data by Gallaway et al. [27] has been selected for this calculation, as demonstrated by Equation (1).

$$d = \left[3.38 \times 10^{-3} \times \left(\frac{1}{T}\right)^{-0.11} \times L^{0.43} \times I^{0.59} \times \left(\frac{1}{S}\right)^{0.42}\right] - T \quad (1)$$

Where, d is water depth above top of texture, which is defined as WFT in this study [in.]; T is the average texture depth [in.]; L is drainage-path length [ft]; I is rainfall intensity [in./h]; S is cross slope [ft/ft].

The selected formula relates the water depth above the top of the pavement texture to average texture depth, drainage-path length, rainfall intensity, and cross slope. In this study, this water depth above the pavement texture is referred as WFT (Fig. 1).

According to Equation (1), an increase in average texture depth results in a lower WFT over the pavement surface. The longer the drainage-path length, the higher the WFT. Greater rainfall intensities lead to an increase in WFT over the pavement surface, while an increase in cross slope results in a reduced WFT.

3.2. WFT calculation model on rutted pavement surface

It is widely acknowledged that pavement rutting can lead to driving safety issues, such as hydroplaning and skidding, as rutting alters the surface runoff of water, leading to reduced tire-pavement friction. Although the adverse effects of pavement rutting on driving safety are well-known, there has been limited research quantifying this risk. When a vehicle travels at a certain speed on a particular pavement surface, the impact of RD can be viewed as an increase in the vehicle's braking distance. Previous studies have shown that during intense rainfall, the pair of ruts tends to become fully filled with water [12,21], with runoff directed toward the road's lateral borders. Along the cross slope (Fig. 2), the WFT on the road border is higher than at any other position.

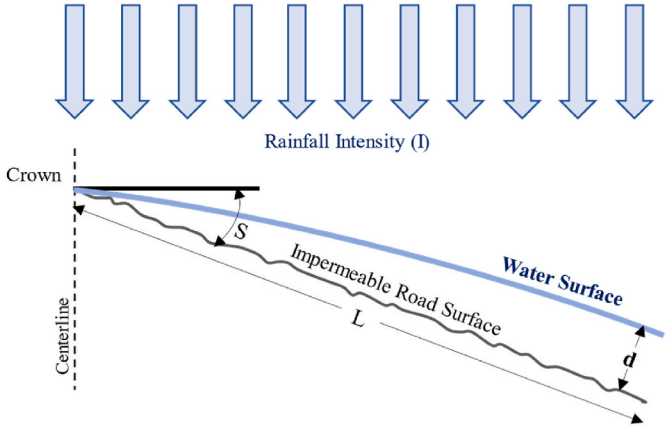

Fig. 1. Diagrammatic representation of water flow over an impermeable road surface [27].

Additionally, a constant RD at all positions within the rut has been considered in this study.

Consequently, sub-model 2 calculates the accumulated WFT within the rut as the sum of RD and the WFT on the undeteriorated pavement surface, as demonstrated by Equation (2).

$$WFT_{rut} = WFT_{surface} + RD \quad (2)$$

where, WFT_{rut} represents the height of the water surface to the bottom of the rut; RD denotes the depth of the rut, which is assumed to be constant; $WFT_{surface}$, represents the WFT over the non-deteriorated road pavement surface.

By integrating Equations (1) and (2), Equation (3) can be obtained, which relates rainfall intensity, average pavement texture depth, number of lanes, lane width, and cross slope in the proposed model.

$$WFT_{rut} = \left[3.38 \times 10^{-3} \left(\frac{1}{T}\right)^{-0.11} L^{0.43} I^{0.59} \left(\frac{1}{S}\right)^{0.42}\right] - T + RD \quad (3)$$

Table 1 indicates the thresholds for RD severity classification as defined by various highway agencies. Based on the sources mentioned below, rut severity is categorized into three clusters: low, medium, and high, which are also adopted in this study.

3.3. Predictive model of dynamic skid resistance using AI machine learning algorithms

Understanding the skid resistance state of a pavement is crucial for assessing the braking distance on that pavement. Once the skid resistance performance of a pavement is predicted, the braking distance for any vehicle speed and WFT can be calculated. Therefore, it becomes essential to assess the skid resistance effectively for any boundary conditions (i.e., WFT and vehicle speed) through sub-model 3.

The first step involves inputting scattered published skid resistance data corresponding to WFT (0–10 mm) and vehicle speed (20–100 km/h) from Chu and Fwa's research [14]. However, it's worth noting that establishing the database of skid resistance performance state in Chu and Fwa's skid resistance simulation model is a time-consuming process. Each skid resistance simulation analysis is an extensive iterative procedure, which may take up to several hours on a high-end workstation [14].

In this study, to obtain a skid resistance for any WFT, ranging from 0 to 10 mm, and vehicle speed, ranging from 0 to 100 km/h, a linear interpolation within the MATLAB environment is employed (Fig. 3a). Since these ranges are limited and not covering wider boundary conditions possibilities, a linear extrapolation is adopted to predict the skid resistance at higher WFT levels, ranging from 0 to 35 mm and vehicle speeds, ranging from 0 to 100 km/h. The interpolated data serve as the foundation for extrapolating dynamic skid resistance (Fig. 3b).

However, it's important to note that this method only considers the gradient at the boundary when WFT equals 10 mm. As a result, there are negative predicted values when WFT approaches 35 mm and vehicle speed approaches 100 km/h. Given that skid resistance is always a positive value, the linear extrapolation model cannot be accepted as input for calculating vehicle braking distance. Therefore, two types of AI Machine Learning algorithms are employed and compared to predict the dynamic skid performance.

The first adopted AI Technique is RF regression analysis, which is an ensemble learning technique that combines multiple decision trees to predict dynamic skid resistance when the WFT exceeds 10 mm (i.e., 10–35 mm). As the first step, the database generated by linear interpolation (Fig. 3a) is inputted and all variables (i.e., WFT and vehicle speed) used in this study are identified. Then, the entire database (with a total of 4572 samples) is divided into separate training and testing datasets, with 80 % allocated to the training dataset (3728 samples) and 20 % to the testing dataset (844 samples). Typically, 80 % of the database is used for training to ensure a sufficiently large dataset for model

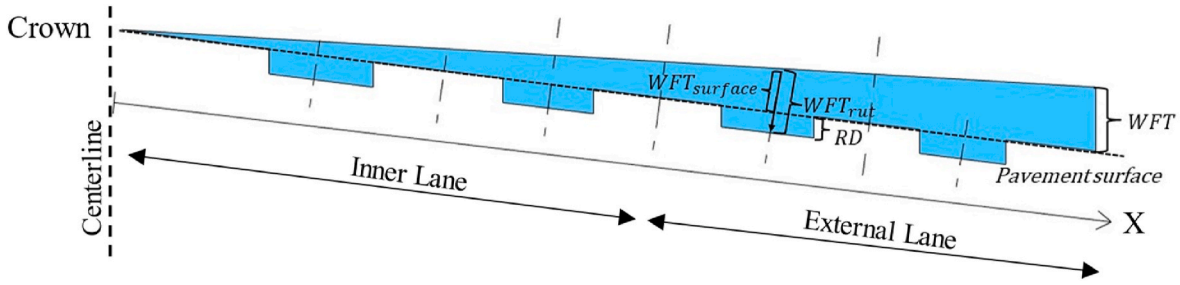

Fig. 2. Schematic diagram of accumulated WFT within the rut and at the road border.

Table 1
Rut severity classification by highway agencies [28–31].

Highway agency	Low [mm]	Medium [mm]	High [mm]
Pavement Condition Index [28]	6.3–12.7	12.7–25.4	>25.4
Washington State Department of Transportation [29]	6.3–12.7	12.7–19.1	>19.1
Ohio Department of Transportation [30]	3.2–9.5	9.5–19.1	>19.1
Ministry of Transportation & Infrastructure, British Columbia [31]	3–10	10–20	>20
Average	4.7–11.2	11.2–20.9	>20.9

training, while the remaining 20 % is reserved for testing to validate the model's predictive performance.

On the second step, RF regression randomly selects features from the dataset to build each tree. Each tree is trained on a random subset of the original database. During the training process, each node of the tree is split based on the best feature and split point found among a random subset of features. A leaf node represents the end node of a decision tree. In this study, the number of trees at 100 is set, with a minimum of 5 samples per leaf.

In the last phase, once the forest is built, predictions are made by aggregating the predictions of all the individual trees. For regression tasks, the most common aggregation method involves taking the average of the predicted values from all the trees. Finally, the performance of the RF regression model is evaluated using the coefficient of determination (R^2), as demonstrated by Equation (4), and Mean Absolute Error (MAE), as calculated by Equation (5).

$$R^2 = 1 - \frac{\sum_{i=1}^{m}(Y_i - \widehat{Y}_i)^2}{\sum_{i=1}^{m}(Y_i - \overline{Y}_i)^2} \tag{4}$$

In Equation (4), m represents the size of the dataset; Y_i stands for the individual observed value; $\widehat{Y}_i$ is the predicted output; $\overline{Y}_i$ denotes the mean value of the dataset; R^2 quantitatively describes the accuracy of the predicted model in relation to the variations in the observed values. An R^2 value close to 1 indicates that the predictions align well with the observed data.

$$MAE = \frac{1}{m}\sum_{i=1}^{m}|Y_i - \widehat{Y}_i| \tag{5}$$

In equation (5), *MAE* serves as a parameter to evaluate predictive performance in terms of error accumulation. When MAE approaches 0, it signifies a better predictive performance.

The R^2 value for both the training and testing datasets of the RF regression model is 99.9 %. The MAE values for the training and testing datasets of the RF regression model are 11.7 % and 12.1 %, respectively. The statistical evaluation indicates a good fit between the observations and predictions. This suggests that RF regression models perform well when WFT ranges from 0 to 10 mm, and vehicle speed ranges from 0 to 100 km/h, as shown in Fig. 4a.

However, the primary aim of this study is to predict skid resistance performance within a broader range, where WFT ranges from 0 to 35 mm, and vehicle speed ranges from 0 to 100 km/h. The RF regression model, being relatively simple, is insufficient to capture the variability in WFT under these conditions. Therefore, when expanding the WFT range (e.g., from 10 to 35 mm) while keeping vehicle speed constant, the RF regression model cannot provide accurate predictions. This limitation arises because the model has only two input variables (i.e., WFT and vehicle speed) and the extension of skid performance is too vast for the model to capture the trend in WFT. Therefore, another AI Machine Learning technique is investigated.

The second adopted AI Technique is BPNN, which is a machine learning algorithm used to train artificial neural networks, specifically Multi-Layer Perceptron (MLP). BPNN improves the output by propagating the error backward and calculating the gradient of the cost function for each weight. The input database (with a total of 4572 samples) is also generated through linear interpolation (Fig. 3a) and then divided into separate training and testing datasets, with 80 % (3728

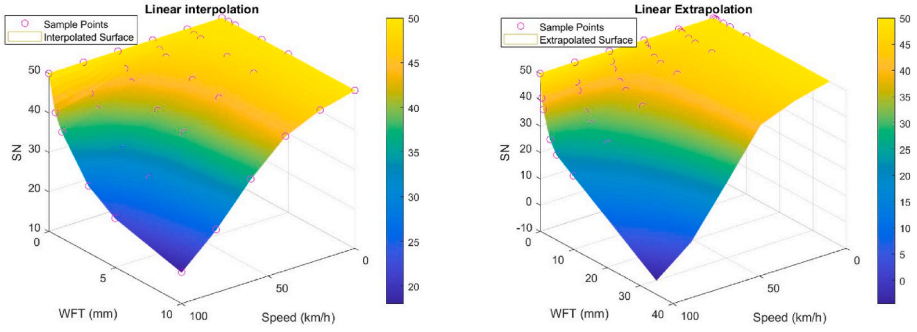

(a) (b)

Fig. 3. Skid resistance performance in MATLAB environment: (a) linear interpolation for WFT ranges from 0 to 10 mm, (b) linear extrapolation for WFT ranges from 0 to 35 mm.

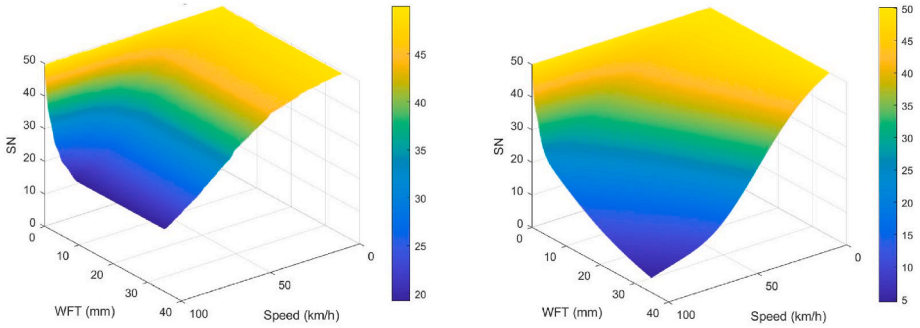

Fig. 4. Skid resistance performance in AI Machine Learning algorithms: (a) RF regression Method, (b) BPNN Method.

samples) allocated to training and 20 % (844 samples) to testing datasets. Fig. 5 illustrates the BPNN framework used in this study.

The input layer comprises WFT and vehicle speed, while there are two hidden layers with 5 and 4 artificial neurons, respectively. The model's output is the prediction of Skid Number (SN) corresponding to each WFT, and vehicle speed. The R^2 values for both the training and testing datasets of the BPNN model is 99.9 %. The MAE values for the training and testing datasets of BPNN are 8 % and 9 %, respectively. Fig. 4b displays the predicted skid performance results using BPNN. For instance, when WFT is 35 mm and vehicle speed is 100 km/h, BPNN predicts an SN value of 4.5. This prediction is acceptable for use as input in calculating vehicle braking distance on wet and rutted pavement surfaces in sub-model 4.

3.4. Calculation model for vehicle braking distance on wet and rutted pavement

The first step involves determining whether the vehicle wheels are positioned within the rut path. If the vehicle wheel is located at the Rutting Position (RP), then the RD affects the vehicle braking distance. Otherwise, rutting has no impact on the vehicle's operation. Vehicle Track Width (VTW) is the distance measured across an axle from the centerline of one tire tread to the centerline of the opposite tire tread. The centerline of the lane refers to the middle line of the lane along the longitudinal direction, dividing it into two halves. This study aims to analyze the impact of RD on vehicle braking distance during rainy days. Therefore, the core assumption in this framework is that VTW/2 equals RP.

In the second step, the accumulated WFT over the pavement surface is determined based on the outputs from sub-models 1 and 2. Sub-model 1 provides data on rainfall intensity, average texture depth, number of lanes, lane width, and cross slope, which are used to calculate WFT over the undeteriorated pavement surface. Sub-model 2 extends this calculation by considering the additional impact of RD on the accumulated WFT over the rutted pavement position. Consequently, inputs for this step include rainfall intensity, average texture depth, number of lanes, lane width, cross slope, and RD to pave the way for the subsequent analysis.

The third step involves predicting skid resistance performance, considering WFT, ranging from 0 to 35 mm, and vehicle speed, ranging from 0 to 100 km/h. In this step, BPNN algorithms is adopted to input *S*N-V-WFT data into the proposed model.

In the final step, the vehicle braking distance can be obtained by combining all the input parameters. This comprehensive algorithm for vehicle braking distance computation is executed within the MATLAB environment. The initial condition at $t = 0$ represents the time when the driver initiates the vehicle's braking process. The initial input, $v(t_1) = v_b$, indicates the vehicle speed at the beginning of braking. Subsequently, an incremental "for-loop" is employed to accumulate the braking distance, step by step, until the condition $v(t_2)>0$ is no longer met, which means the vehicle comes to full stop. As a result of this "for-loop" algorithm, the output is the vehicle's braking distance required to stop on rutted and wet pavement.

Fig. 6 illustrates the overall framework for computing vehicle braking distance through sub-model 4, considering various factors including weather conditions, vehicle speed, pavement conditions, WFT, road geometry, and RD.

4. Model validation and calibration

4.1. Model validation

Validating the results from the developed model is crucial for assessing the precision of the outcomes. It's important to note that there are no existing identical models in the literature that can evaluate vehicle braking distance on road pavement under the influence of both wet and rutted conditions. This underscores the innovation of this study. However, it is possible to find similar models that calculate vehicle braking distance under dry conditions and within limited ranges of WFT [14,32]. Therefore, three different approaches are adopted in the validation process, as explained in the following.

- Comparing the results of the proposed model on dry pavement with the existing model,
- Comparing the results of the proposed model on wet pavement with the existing model,
- Comparing the results of wet pavement conditions with dry pavement conditions in the proposed model of this study.

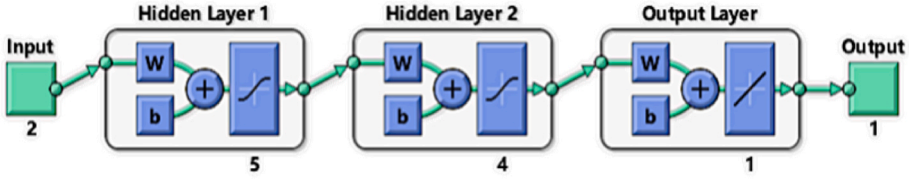

Fig. 5. Adopted framework of BPNN exclusive to this study.

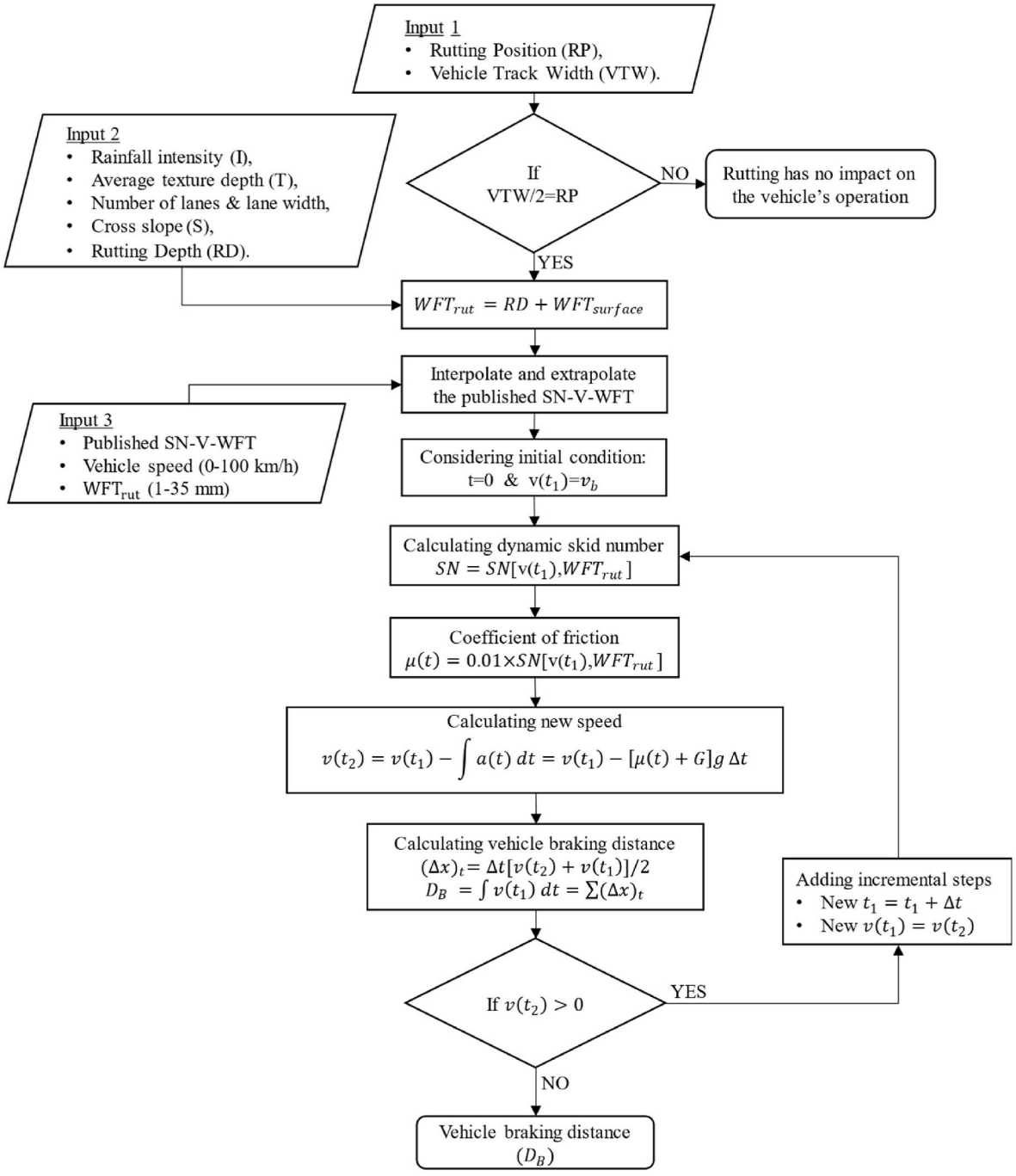

Fig. 6. The framework of vehicle braking distance simulation model on wet and rutted pavement.

4.1.1. Validation according to existing model on dry pavement

The first validation consists of restimulating the predefined conditions available in existing literature (as per the Australian Standard [32]), using the proposed model in this study for calculating vehicle braking distance on dry road pavement. In the Australian Standard, the vehicle braking distance on dry road pavement is calculated using Equation (6), with the definitions of v, μ, and g listed in Table 2.

$$braking\ distance = 0.039 \times \frac{v^2}{\mu g} \tag{6}$$

After re-simulating the illustrative example of the Australian standard on dry pavement using the proposed model in this study, with a given SN_0 of 50, a given vehicle speed of 50 km/h, and a WFT of 0 mm, the comparison yielded the following results: the simulated vehicle braking distance by the proposed model in this study was 19.66 m, while the Australian standard's result was 19.9 m [32]. The relative error between them is only 1.21 %, which is the first proof of the reliability of the proposed model.

Table 2
Boundary conditions adopted by Australian Standard [32].

Adopted parameters	Values
μ: Coefficient of Friction in dry condition for cars	0.50
v: design speed [km/h]	50
g: gravitational acceleration [m/s^2]	9.81

4.1.2. Validation according to existing model on wet pavement

The second validation consists of restimulating the predefined conditions available in existing literature (as proposed by Chu and Fwa [14]), for calculating vehicle braking distance on wet road pavement. Three illustrative examples from Chu and Fwa's model are re-simulated, with the input boundary conditions as presented in Table 3.

Table 4 displays the relative error between the re-simulation conducted using the proposed model and the results from the literature, which falls within an acceptable range.

As it can be interpreted from Table 4, it can be declared that also the second validation approach proofs the validity of the proposed model. These validations not only confirm the legitimacy of the proposed model but also address the limitations observed in prior studies. Specifically, the shortcomings related to the insufficient coverage of limited WFTs and the lack of consideration for the coupled effect with RD can now be effectively resolved through the application of the proposed model.

4.1.3. Validation according to proposed model on dry and wet pavement surfaces

The third validation involves comparing the results of wet pavement conditions (i.e., WFT = 1.5 mm) with dry pavement conditions (i.e., WFT = 0 mm) using the proposed model in this study. In dry surface conditions, the SN is assumed to be constant with SN_0 equal to 50 for any vehicle speed. However, in the presence of water, dynamic SN values corresponding to specific vehicle speeds must be calculated from the skid resistance state surface developed in sub-model 3. The results, as shown in Fig. 7, indicate that the proposed model, as expected, is sensitive to the presence of water, resulting in increased braking distances.

4.2. Model calibration

Due to the presence of a transversal slope, the WFT at the left wheel position is lower than that at the right wheel position, implying that the skid resistance at the left wheel position is greater than at the right wheel position. Consequently, the braking distance for the left wheel is shorter than that for the right wheel. To calibrate this model, an average braking distance is computed between the left wheel and the right wheel using Equation (7).

$$D_B = \left(D_B^{left} + D_B^{right}\right)/2 \tag{7}$$

After calibrating the proposed model, the same illustrative examples are re-simulated. Vehicle braking distance decreases, indicating that the proposed model is sensitive to the WFT, resulting in slightly shorter vehicle braking distances, as shown in Table 5.

5. Sensitivity analysis: results and discussion

To study the impact of each input parameter available for different lanes on vehicle braking distance under wet and rutted pavement conditions, several sensitivity analyses are conducted using the proposed model in this study. A simple road section with two lanes per direction (Fig. 8) is selected for these sensitivity analyses. Both the 1st and 2nd lanes have a lane width of 3.5 m. The cross slope is set at 2.5 % in sections 5.1, 5.2, and 5.4, while the sensitivity analysis related to cross slope is performed in section 5.3, considering cross slopes of 2.5 % and 7 %. The average texture depth is 0.127 mm (0.005 in.), and the vehicle track width is 1.5 m. A rainfall intensity of 100 mm/h is considered as the intense weather condition for the simulation.

Table 3
Boundary conditions adopted by Chu and Fwa [14].

Inputted Boundary Conditions	Values
$V_{t=0}$: vehicle speed at time 0	90, 80, 50 [km/h]
$SN(V_{t=0})$: SN at vehicle speed at time zero	50
$\mu(t=0)$: friction coefficient at time zero	0.50
Δt: numerical integration time step	0.1 [s]
G: roadway grade	0 [%]
g: gravitational acceleration	9.81 [m/ s^2]
w: water film thickness	0.5, 3, 8 [mm]

5.1. Impact of variable RDs and vehicle speeds on the braking distance

The first scenario considers RD and vehicle speed at the time of braking initiation as variables but maintains the lane, WFT, and cross slope as constant parameters. Fig. 9 illustrates the vehicle braking distance on the external lane under different pavement deterioration conditions with varying RDs (ranging from 0 to 25 mm) and various WFT layers existing on different parts of the road surface. These predicted braking distances correspond to specific vehicle speeds (i.e., 50, 60, 70, 80, 90, 100 km/h) at the moment of braking initiation. WFT on the road surface is determined by factors such as rainfall intensity, cross slope, mean texture depth, the number of lanes per direction, and lane width, as calculated by sub-model 1. An RD value of 0 indicates the absence of rut over the pavement.

In Fig. 9, the vehicle braking distance exhibits a gradual rise with an increase in RD (Rainfall Depth) at a consistent vehicle speed. This observed trend is attributed to the diminishing skid resistance of wet and rutted pavement surfaces associated with the growing RD. It's crucial to emphasize that, at each designated vehicle speed, the vehicle braking distance experiences an accelerating escalation in tandem with the rising RD. This acceleration is directly linked to the declining skid performance, a correlation illustrated in Fig. 4b. As an example, for a vehicle speed of 70 km/h, AASHTO [33] recommends that the braking distance should be 56.2 m, while the simulated vehicle braking distance by proposed model is 42.8 m on wet pavement without rutting. As RD increases to 5, 10, 15, 20, and 25 mm, the vehicle braking distance increases by 11 %, 17 %, 27 %, 43 %, and 67 %, respectively.

5.2. Impact of variable lanes, vehicle speeds and WFTs on the braking distance

The second scenario investigates lane, WFT, and vehicle speed variations on the braking distance. According to sub-model 1, the WFT on the external lane is thicker than the WFT on the inner lane at the same non-deteriorated road cross section. Consequently, the vehicle's braking distance on the external lane is longer than on the inner lane since the tire-pavement interaction is less. Fig. 10 illustrates the vehicle's braking distance with different vehicle speeds and WFT levels, allowing a comparison between the simulated scenarios on the inner and external lanes. As an example, for a vehicle speed of 70 km/h, the difference in vehicle braking distance is 2 m when the WFT is 5 mm, and 1.6 m when WFT is 10 mm, increasing to 26.5 m for a WFT of 35 mm. This results in percentage increases in vehicle braking distance of 4.5 %, 3.5 %, and 45.8 % for WFT values of 5, 10, and 35 mm, respectively. It can be observed graphically that there is a sudden change of vehicle braking distance increasing trend for a WFT threshold value of 10 mm, this is due to the changing of gradient in skid performance as shown in Fig. 4b.

5.3. Impact of variable cross slopes, vehicle speeds and WFTs on the braking distance

Cross slope is another important influencing factor in determining the vehicle braking distance on wet and rutted pavements. Therefore, as the third scenario, the value of RD and the understudy lane are considered as constant parameters, while the cross slope, WFT level, and vehicle speed are variables. Fig. 11 illustrates the vehicle braking distance with different vehicle speeds on various WFT levels regarding the external road lane, allowing a comparison between the simulated scenarios on the 2.5 % and 7 % cross slopes.

According to Fig. 11, it is important to emphasize that increases in road cross slope result in reduction of water depths as the drainage

Table 4
Comparison of braking distances between the literature [14] and the proposed model.

SN_0	Braking distance by Chu and Fwa [14]			Braking distance by proposed model			Relative error [%]
	WFT [mm]	Vehicle speed [km/h]	Braking distance [m]	WFT [mm]	Vehicle speed [km/h]	Braking distance [m]	
50	0.5	90	70.3	0.5	90	69.94	0.51
	3	80	59.4	3	80	61.96	4.13
	8	50	21.6	8	50	21.93	1.53

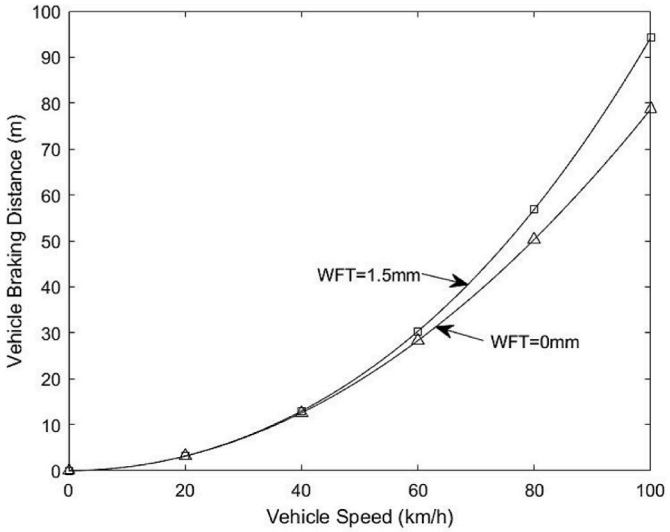

Fig. 7. Illustrative results of wet pavement conditions (WFT = 1.5 mm) and dry pavement conditions (WFT = 0 mm) simulated using the proposed model in this study.

Table 5
Simulated examples result before and after model calibration.

SN_0	WFT [mm]	Vehicle speed [km/h]	Braking distance before calibration [m]	Braking distance after calibration [m]	Variation percent [%]
50	0.5	90	69.94	68.45	−3.13
	3	80	61.96	59.53	−3.92
	8	50	21.93	21.83	−0.46

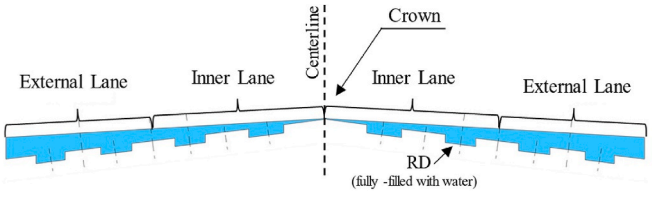

Fig. 8. Schematic diagram of 2-lane road cross section.

process happens faster. Therefore, flatter road section leads to longer vehicle braking distances. As an example, for a vehicle speed of 70 km/h, the vehicle braking distance difference is 1.7 m when the WFT is 5 mm, and 1.4 m when the WFT is 10 mm, increasing to 25.4 m for a WFT of 35 mm. The corresponding percentage increase in vehicle braking distance is 3.8 %, 2.9 %, and 43.1 % for WFT values of 5, 10, and 35 mm.

6. Confronting rutting severity thresholds with AASHTO braking distance requirements

For illustrative purposes, three rutting severity threshold levels (i.e., low, medium, high) adopted by several highway agencies are simulated

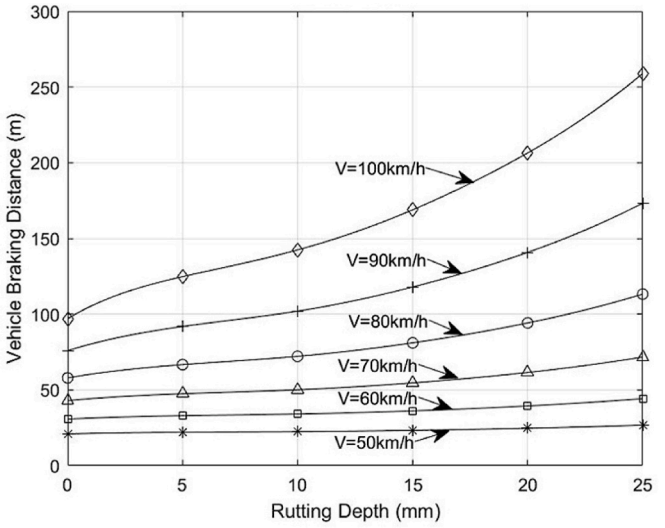

Fig. 9. Vehicle braking distance corresponding to various RD and vehicle speed.

and examined with the proposed model in this study and the results are compared to the accepted braking distances at each vehicle speed, required by AASHTO [33]. For this matter, a set of boundary conditions are considered as explained in Fig. 12. This figure displays the predicted braking distances by the proposed model according to the average threshold levels set by four highway agencies for low, medium, and high rutting severities, which are 4.7–11.2 mm, 11.2–20.9 mm, and >20.9 mm, respectively.

As demonstrated by the figure, the vehicle braking distance on wet and rutted pavement increases with higher vehicle speed, which aligns with expectations. In other words, the vehicle speed is directly proportional to vehicle braking distance, as demonstrated in sub-model 4. The rate of increase in vehicle braking distance becomes notably steeper when the vehicle speed surpasses approximately 60 km/h. For a RD of 4.7 mm, the vehicle braking distance increases by 90.8 m when the vehicle speed increases from 60 to 100 km/h, while the corresponding increases are 113.4 and 174.5 m for RD values of 11.2 and 20.9 mm, respectively.

Graphical analysis reveals a comparison between the estimated braking distances on the wet and rutted pavement surface and the AASHTO required braking distance under dry and non-deteriorated pavement conditions. It can be seen that the effect of various rut severity on vehicle braking distance can be negligible when the vehicle speed is lower than 60 km/h. However, when the vehicle speed exceeds 60 km/h, RD contributes significantly to the results of vehicle braking distance. Depending on the rut severity and vehicle speed there is a region where the braking distance requirements are met. To illustrate, for a low rut severity threshold, the vehicle speed must not exceed 80 km/h; for a medium rut severity threshold, the vehicle speed must not exceed 60 km/h to meet the safe braking requirements. According to Fig. 12, the area above the AASHTO requirements may be considered as a risk zone.

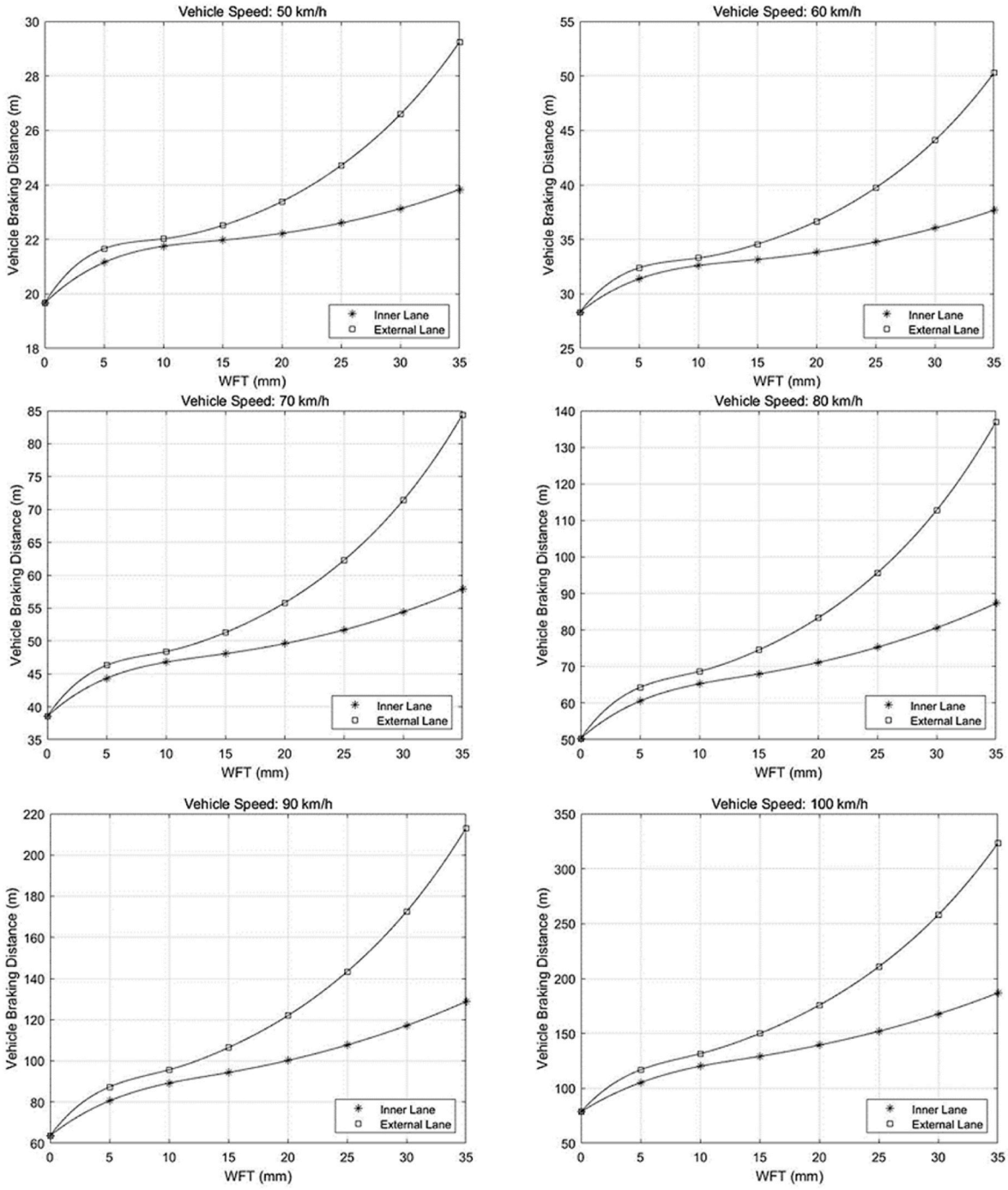

Fig. 10. Vehicle braking distance corresponding to various road lanes scenarios (i.e., inner/external lane).

7. Conclusions

This study introduces an analytical model, based on AI Machine Learning, for calculating vehicle braking distance under wet and rutted pavement conditions. The model considers various factors, including rainfall intensity, number of lanes, lane width, cross slope, average texture depth, rutting depth, accumulated water film thickness, and a wide range of vehicle speeds. The outcomes of this model underscore the following points.

- An investigation of the best-fitted Machine Learning algorithm to train the existing but limited dynamic skid resistance in literature,
- An effective prediction of dynamic skid resistance in the tire-pavement interaction, accomplished through Back-Propagation Neural Network (BPNN) with rapid computation times,
- The quantitative assessment of the influence of rutting depth on vehicle braking distance under wet road pavement conditions,
- The correlation between AASHTO braking distance requirements and the simulated vehicle braking distance for permissible rutting depth across different vehicle speeds,
- A precise estimation of vehicle braking distance on wet and rutted road pavement.

It is worth noting that the wide and reliable prediction of dynamic skid resistance, achieved through the application of a Machine Learning

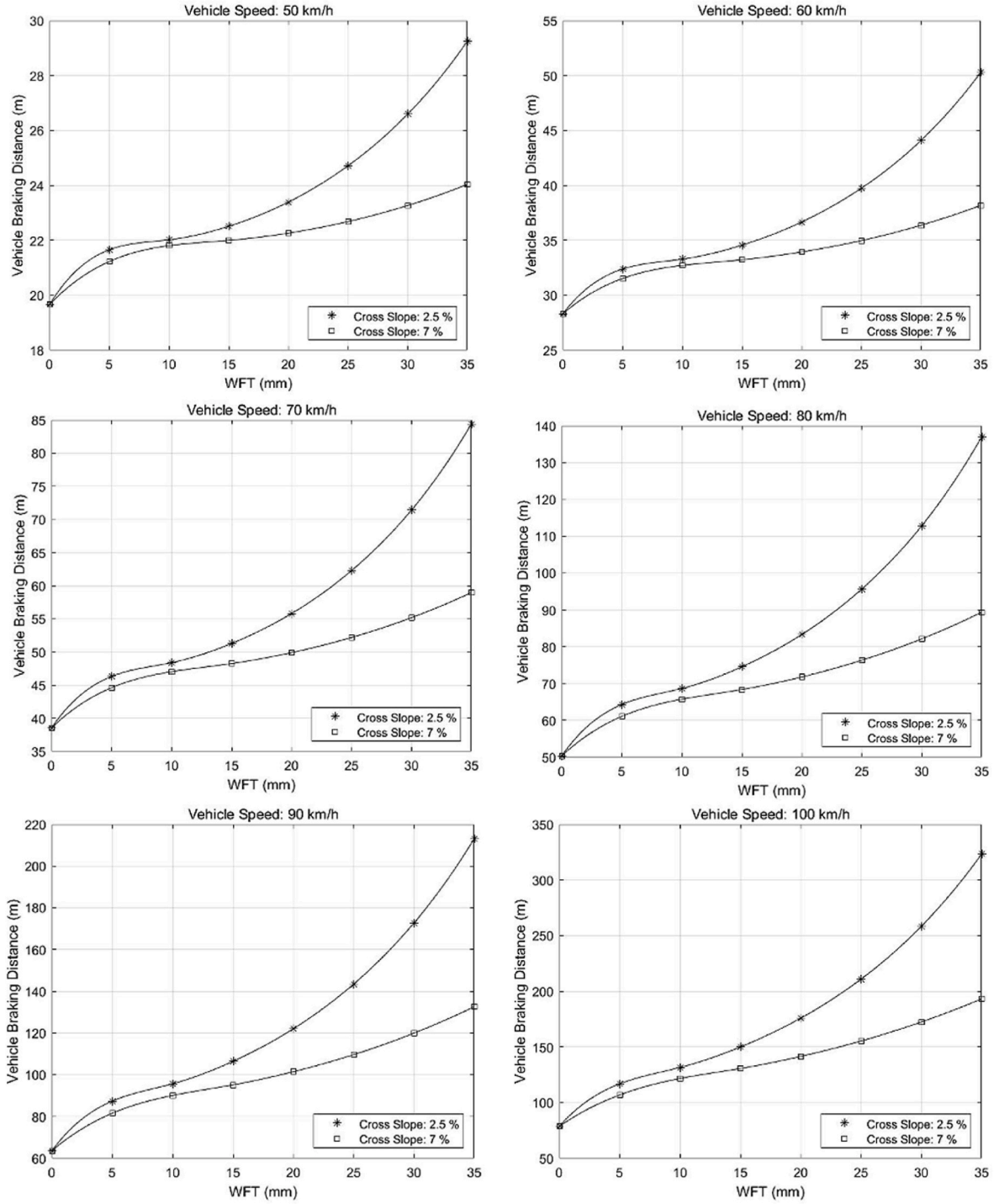

Fig. 11. Vehicle braking distance corresponding to various cross slope scenarios (i.e., 2.5 % and 7 %).

method in this study, is a novel contribution not found in previous literature. While there exist analytical models for predicting pavement skid resistance performance, the process of establishing a database of skid resistance performance states is notably time-consuming. With the model proposed in this study, skid resistance prediction, employing Back-Propagation Neural Network (BPNN) in the MATLAB environment, takes only a matter of seconds. Subsequently, the obtained dynamic skid resistance data can be directly utilized as input for calculating vehicle braking distances on wet and rutted pavements.

Furthermore, this model integrates the influence of weather conditions, pavement conditions, and road geometry into the evaluation of vehicle braking distances. The results obtained from this study also allow for the assessment of how cross slope, the number of lanes, and lane width affect vehicle braking distances on wet and rutted pavements.

As indicated in this study, a key input for the proposed model is information concerning the depth of rutting along the road section. The accuracy of the results generated by this model hinges on the availability of pavement condition data and, subsequently, the frequency of survey execution. In essence, to achieve predictions closely aligned with the actual vehicle performance on the pavement, real-time pavement condition data is crucial. Regrettably, this demand is not always met due to

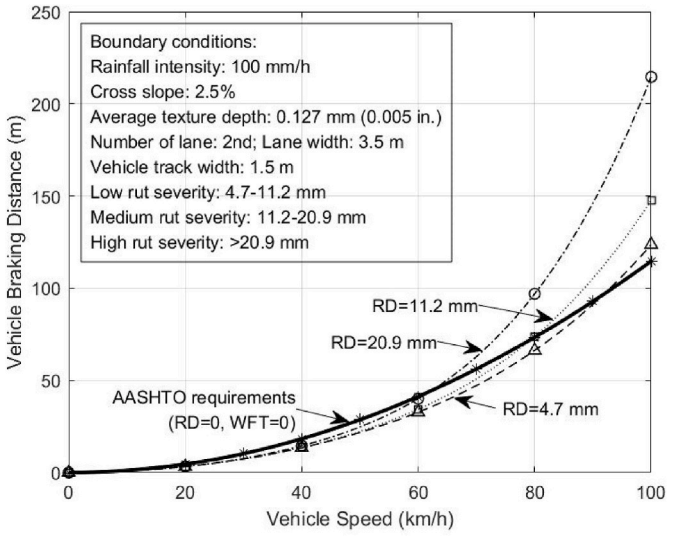

Fig. 12. Confrontation of rutting thresholds with AASHTO braking distance requirements.

challenges such as the time-consuming and expensive nature of obtaining such information.

It is worth emphasizing that by furnishing the proposed model with real-time pavement condition information, including precise data derived from on-site rutting tests, it becomes feasible to predict the performance of vehicles on the studied road section. This predictive capability represents a fundamental step in assessing the operational risks associated with the road. Furthermore, this information is essential for equipping road engineers with valuable insights into the pavement's performance throughout its useful lifespan. This, in turn, enables the scheduling of appropriate maintenance interventions, directly influencing the safety and comfort of road users.

CRediT authorship contribution statement

Jiaqi Jiang: Writing - original draft, Validation, Software, Resources, Investigation, Formal analysis, Data curation. **Misagh Ketabdari:** Writing - review & editing, Writing - original draft, Validation, Software, Resources, Methodology, Investigation, Formal analysis, Data curation, Conceptualization. **Maurizio Crispino:** Supervision, Project administration. **Emanuele Toraldo:** Writing - review & editing, Validation, Supervision, Project administration, Methodology, Conceptualization.

Declaration of competing interest

The authors declare that they have no known competing financial interests or personal relationships that could have appeared to influence the work reported in this paper.

Data availability

Data will be made available on request.

Acknowledgements

There is no conflict of interest to disclose. This research did not receive any specific grant from funding agencies in the public, commercial, or not-for-profit sectors.

References

[1] M.W. Hancock, B. Wright, A Policy on Geometric Design of Highways and Streets, American Association of State Highway and Transportation Officials, Washington, DC, USA, 2013, p. 3.
[2] C.G. Giles, B.E. Sabey, K.H.F. Cardew, Development and performance of the portable skid resistance tester, Rubber Chem. Technol. 38 (4) (1965) 840–862.
[3] W.B. Horne, J.A. Tanner, Joint NASA-British Ministry of Technology skid correlation study-Results from American vehicles, Pavement Grooving and Traction Studies 1969 (1969).
[4] J.J. Henry, Tire Wet-Pavement Traction Measurement: A State-Of-The-Art Review, ASTM International, 1986, pp. 47–60.
[5] M.C. Leu, J.J. Henry, Prediction of skid resistance as a function of speed from pavement texture measurements, Transport. Res. Rec. 666 (2) (1978) 7–13.
[6] J.G. Rose, B.M. Gallaway, Water depth influence on pavement friction, Transp. Eng. J. ASCE 103 (4) (1977) 491–506.
[7] T.F. Fwa, G.P. Ong, Wet-pavement hydroplaning risk and skid resistance: analysis, J. Transport. Eng. 134 (5) (2008) 182–190.
[8] G.P. Ong, T.F. Fwa, Wet-pavement hydroplaning risk and skid resistance: modeling, J. Transport. Eng. 133 (10) (2007) 590–598.
[9] G.P. Ong, T.F. Fwa, Prediction of wet-pavement skid resistance and hydroplaning potential, Transport. Res. Rec. 2005 (1) (2007) 160–171.
[10] G.P. Ong, T.F. Fwa, Modeling skid resistance of commercial trucks on highways, J. Transport. Eng. 136 (6) (2010) 510–517.
[11] G.P. Ong, T.F. Fwa, Mechanistic interpretation of braking distance specifications and pavement friction requirements, Transport. Res. Rec. 2155 (1) (2010) 145–157.
[12] L. Chu, T.F. Fwa, G.P. Ong, Evaluating hydroplaning potential of rutted highway pavements, J. Eastern Asia Soc. Transport. Studies 11 (2015) 1613–1622.
[13] T.F. Fwa, Determination and prediction of pavement skid resistance–connecting research and practice, J. Road Engin. 1 (2021) 43–62.
[14] L. Chu, T.F. Fwa, Incorporating braking distance evaluation into pavement management system for safe road operation, Transport. Res. Rec. 2639 (1) (2017) 119–128.
[15] H.R. Pasindu, T.F. Fwa, G.P. Ong, Computation of aircraft braking distances, Transport. Res. Rec. 2214 (1) (2011) 126–135.
[16] W.B. Horne, T.J. Yager, G.R. Taylor, Recent Research to Improve Tire Traction on Water, Slush and Ice, Publication, 1965, 83984, 66.
[17] M. Ketabdari, M. Crispino, F. Giustozzi, Probability contour map of landing overrun based on aircraft braking distance computation, in: Pavement and Asset Management, CRC Press, 2019, pp. 731–740, https://doi.org/10.1201/9780429264702.
[18] M. Ketabdari, E. Toraldo, M. Crispino, V. Lunkar, Evaluating the interaction between engineered materials and aircraft tyres as arresting systems in landing overrun events, Case Stud. Constr. Mater. 13 (2020), e00446, https://doi.org/10.1016/j.cscm.2020.e00446.
[19] M. Ketabdari, E. Toraldo, M. Crispino, Assessing the impact of the slopes on runway drainage capacity based on wheel/path surface adhesion conditions, Aviation 25 (3) (2021) 140–148, https://doi.org/10.3846/aviation.2021.15329.
[20] Y. Du, J. Chen, Z. Han, W. Liu, A review on solutions for improving rutting resistance of asphalt pavement and test methods, Construct. Build. Mater. 168 (2018) 893–905.
[21] T.F. Fwa, H.R. Pasindu, G.P. Ong, Critical rut depth for pavement maintenance based on vehicle skidding and hydroplaning consideration, J. Transport. Eng. 138 (4) (2012) 423–429.
[22] H.R. Pasindu, T.F. Fwa, G.P. Ong, Analytical evaluation of aircraft operational risks from runway rutting, Int. J. Pavement Eng. 17 (9) (2016) 810–817.
[23] E. Toraldo, M. Ketabdari, G. Battista, M. Crispino, Assessing the impact of rutting depth of bituminous airport runway pavements on aircraft landing braking distance during intense precipitation, Design 7 (2) (2023) 41, https://doi.org/10.3390/designs7020041.
[24] R. Nyirandayisabye, H. Li, Q. Dong, T. Hakuzweyezu, F. Nkinahamira, Automatic pavement damage predictions using various machine learning algorithms: evaluation and comparison, Results in Engineering 16 (2022), 100657.
[25] Z. Pan, S.L. Lau, X. Yang, N. Guo, X. Wang, Automatic pavement crack segmentation using a generative adversarial network (GAN)-based convolutional neural network, Results in Engin. 19 (2023), 101267.
[26] M. Chen, X. Kang, X. Ma, Deep learning–based enhancement of small sample liquefaction data, Int. J. GeoMech. 23 (9) (2023), 04023140.
[27] B.M. Gallaway, R.E. Schiller, J.G. Rose, The Effects of Rainfall Intensity, Pavement Cross Slope, Surface Texture, and Drainage Length on Pavement Water Depths (No. Study No 138), 1971.
[28] M.Y. Shahin, Pavement Management for Airports, Roads, and Parking Lots, vol. 501, Springer, New York, 2005.
[29] Northwest Pavement Management Association, Pavement Surface Condition Field Rating Manual for Asphalt Pavements, Washington State DOT, Olympia, WA, 1999.
[30] Ohio State Dept. of Transportation (ODOT), Pavement Condition Rating System, 2006. Columbus, OH).
[31] British Columbia Ministry of Transportation and Infrastructure (BC MTI), Pavement Surface Condition Rating Manual, third ed., BC MTI, Victoria, BC, 2009.
[32] Urban Road Design, Guide to the Geometric Design of Major Urban Roads, AustRoads, Sydney, Australia, 2002. AP-G69/02.
[33] Transportation Officials, A Policy on Geometric Design of Highways and Streets, 2011, AASHTO, 2011.